



DOE/NSF Thermoelectric Partnership **Project SEEBECK**

**Saving Energy Effectively By Engaging in
Collaborative research and sharing Knowledge**

Joseph P. Heremans (Ohio State University)

Lon Bell (BSST)

Mercouri Kanatzidis (Northwestern University)

Dmitri Kossakovski (ZTPlus)

Guo-Quan Lu (Virginia Polytechnic Institute and State
University)

Ack. Audrey Chamoire, Christopher M. Jaworski

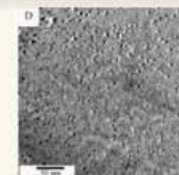
Presentation:

2011 Thermoelectrics Application Workshop, San Diego, Jan 3-6, 2011

Structure of this project

1. Materials

NU – OSU
PbSe –based or
 Mg_2X ($X=Ge, Si, Sn, Pb$)

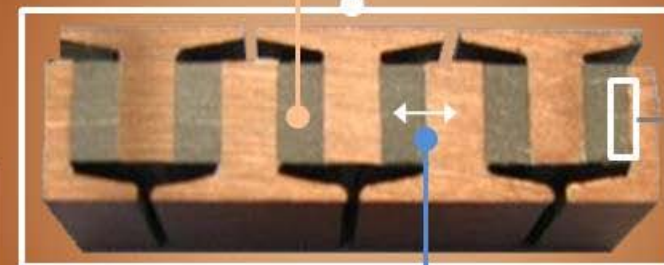


2. Thermal Management

BSST
Innovative
Design and Architecture

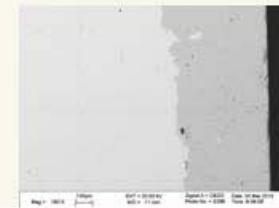
5. Durability

BSST – OSU – NU
VT – ZTPlus
Mechanical and
Thermal shock
resistance



3. Interfaces

VT – ZTPlus
New flexible
Ag Nanopaste and
metallization



4. Metrology

BSST – OSU – NU
VT – ZTPlus
(ITE)
Chemical and Physical
characterization

1. Materials

1.1 PbSe

D. Parker, D. J. Singh "High-temperature thermoelectric performance of PbSe", 29th International Conference on Thermoelectrics, Shanghai, China, May 30-June 3, 2010

1.1.1 Resonant levels

1.1.2 Nanostructuring

1.2 Mg₂(Si, Sn)

1.2.1 Resonant levels

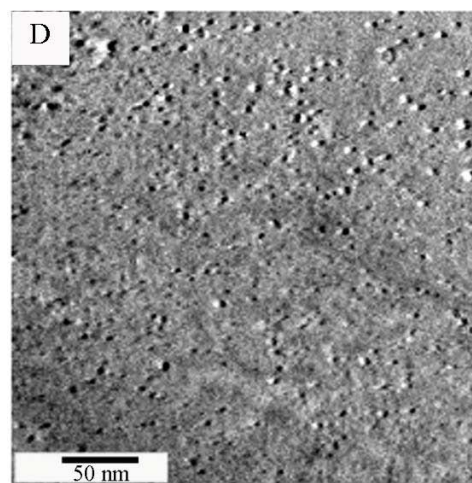
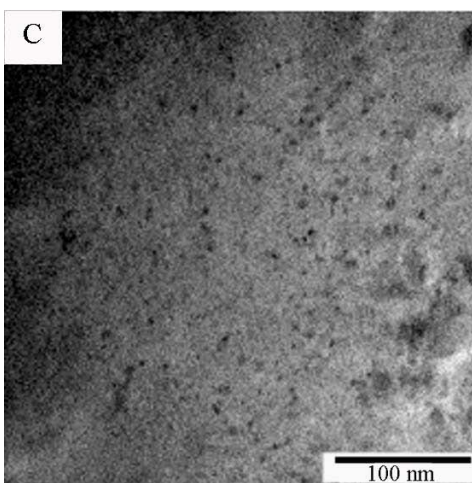
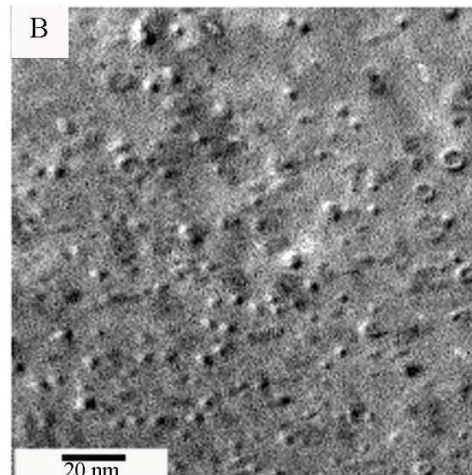
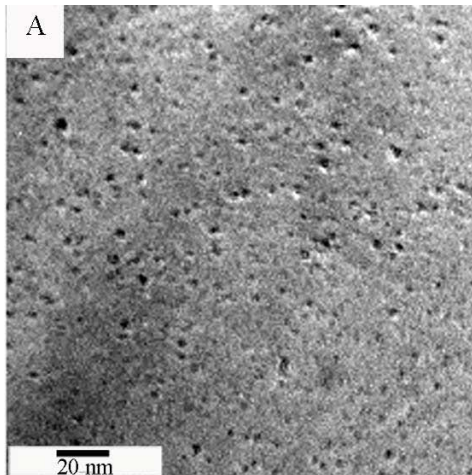
1.2.2 Nanostructuring

Northwestern, OSU

1.1.2 Nanostructuring PbSe

Same bulk solid-state techniques as PbTe

J. R. Sootsman, R. J. Pcionek, H. Kong, C. Uher, M. G. Kanatzidis, "Strong Reduction of Thermal Conductivity in Nanostructured PbTe Prepared by Matrix Encapsulation", Chem. Mater. 18 p.4993 (2006).



Dispersed nanoparticles in samples of Sb-doped PbTe:

- (A) $PbTe-Sb(2\%)$
- (B) $PbTe-Sb(4\%)$
- (C) $PbTe-Sb(8\%)$ and
- (D) $PbTe-Sb(16\%)$.

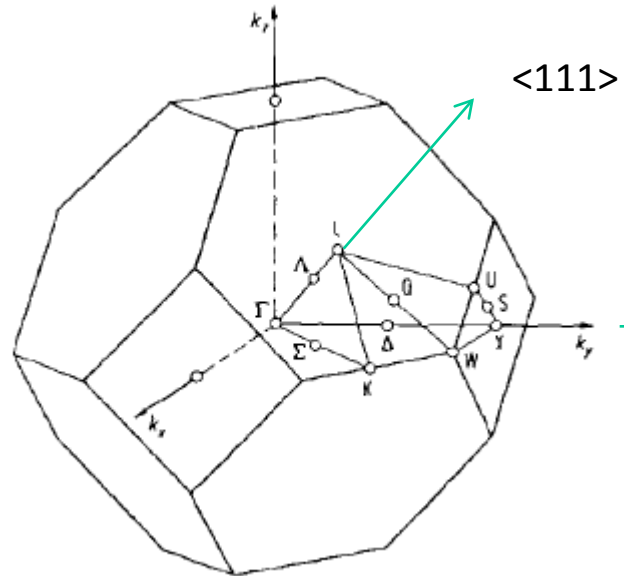
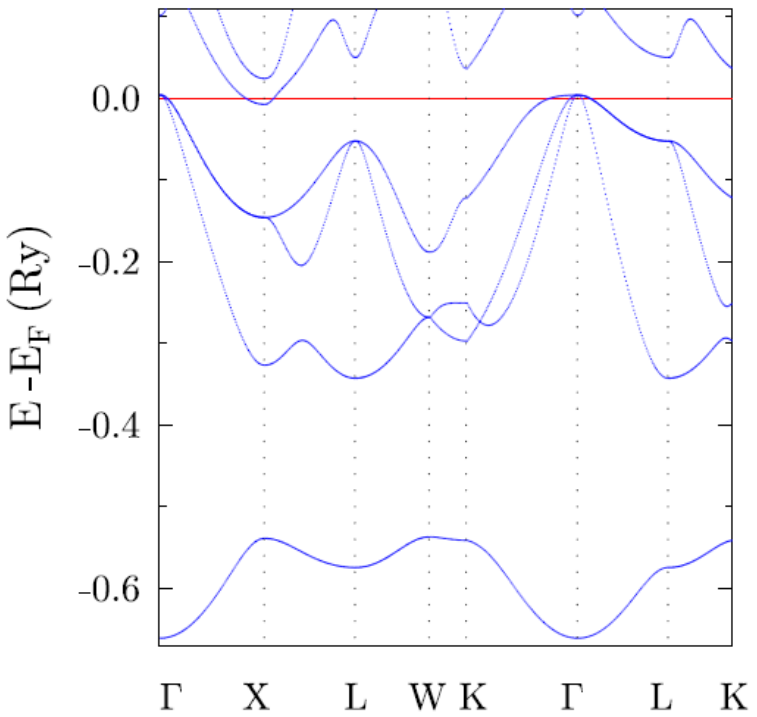
Initial results on PbSe:
 $ZT \sim 0.8$

1.2.1 Resonant levels in $Mg_2(Si, Sn)$

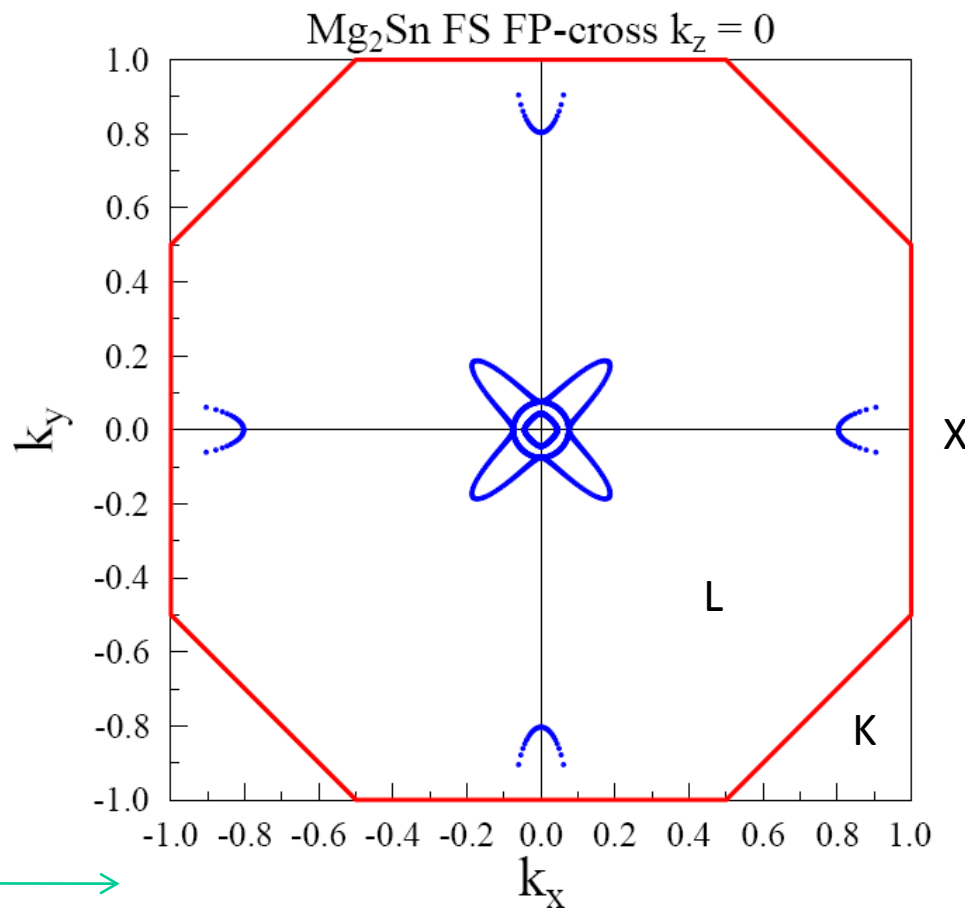
1. Need details of band structure to choose the right level
2. Start from band structure calculations
example(J. Tobola): Ag creates additional DOS in valence band
3. Preliminary experiments: Shubnikov-de Haas measurements on single-crystal Mg_2Sn doped with Ag

Christopher M. Jaworski¹, H.Y. Chen², N. Savvides², B. Wiendlocha³, J. Tobola³, J.P. Heremans^{1,4} Presented at the 2009 International Conference on Thermoelectricity

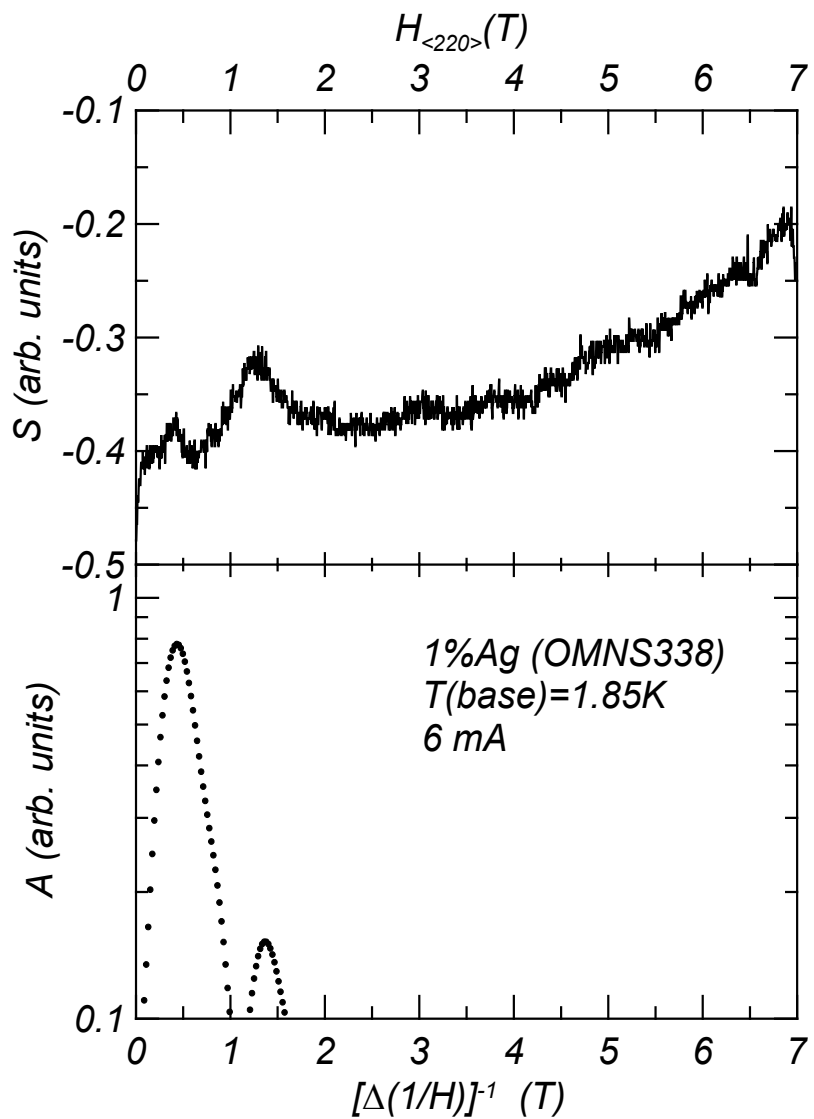
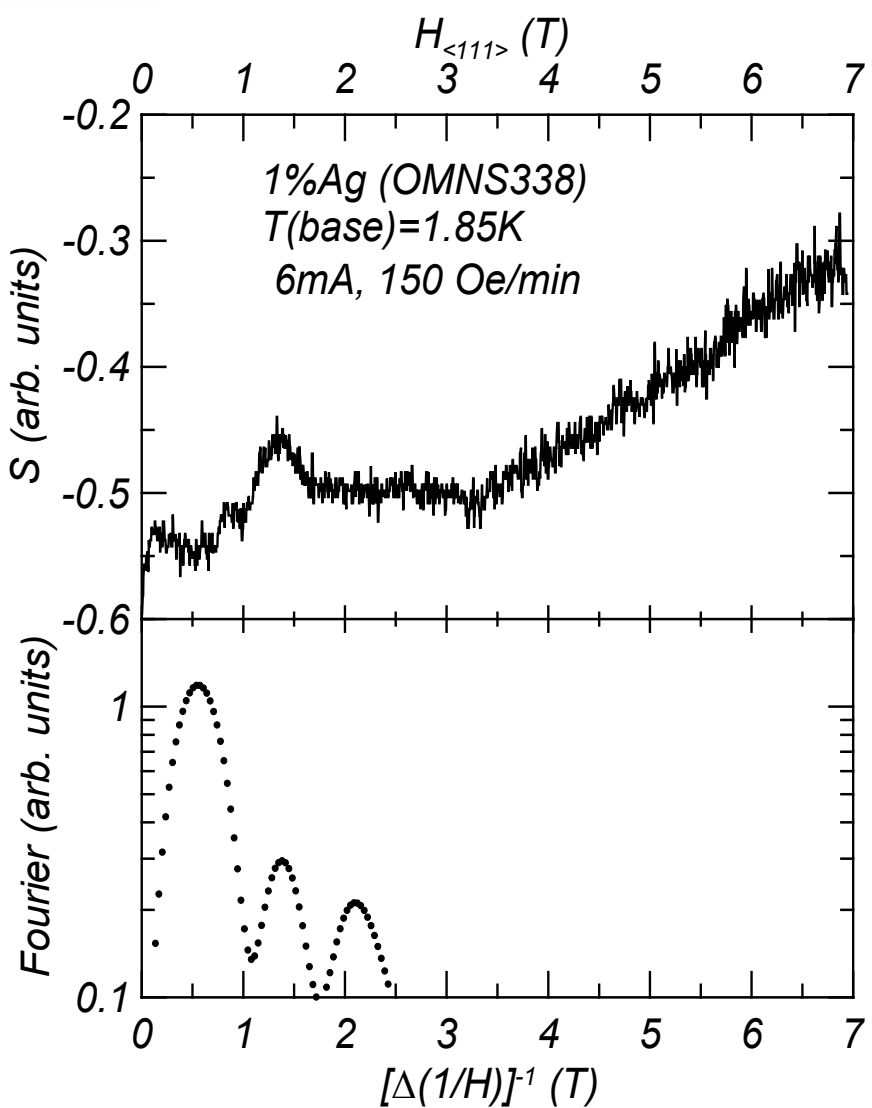
Mg_2Sn (KKR)



Calculated Fermi Surface



Representative Traces 1 % Ag



SdH Oscillations

Ag content (at %)	0.25%	1%
$1/\Delta(1/H)$ (Tesla), $H//<111>$	1.24	0.61
$A_{F,<111>} (m^{-2})$	1.18×10^{16}	0.58×10^{16}
$1/\Delta(1/H)$ (Tesla), $H//<111>$		1.3
$A_{F,<111>} (m^{-2})$		1.2×10^{16}
$1/\Delta(1/H)$ (Tesla), $H//<220>$	0.65	0.61
$A_{F,<220>} (m^{-2})$	0.62×10^{16}	0.58×10^{16}
$1/\Delta(1/H)$ (Tesla), $H//<220>$	1.25	1.378
$A_{F,<220>} (m^{-2})$	1.19×10^{16}	1.31×10^{16}

Possible cyclotron masses from SdH and $E_F(S)$

$$m_c (.25\% \text{ Ag}) = 0.013, 0.025 m_e$$

$$m_c (1\% \text{ Ag}) = 0.005, 0.011 m_e$$

Same result for $<111>$ $<220>$

$$m_c = \frac{\hbar^2 A_F}{\pi 2 E_F}$$

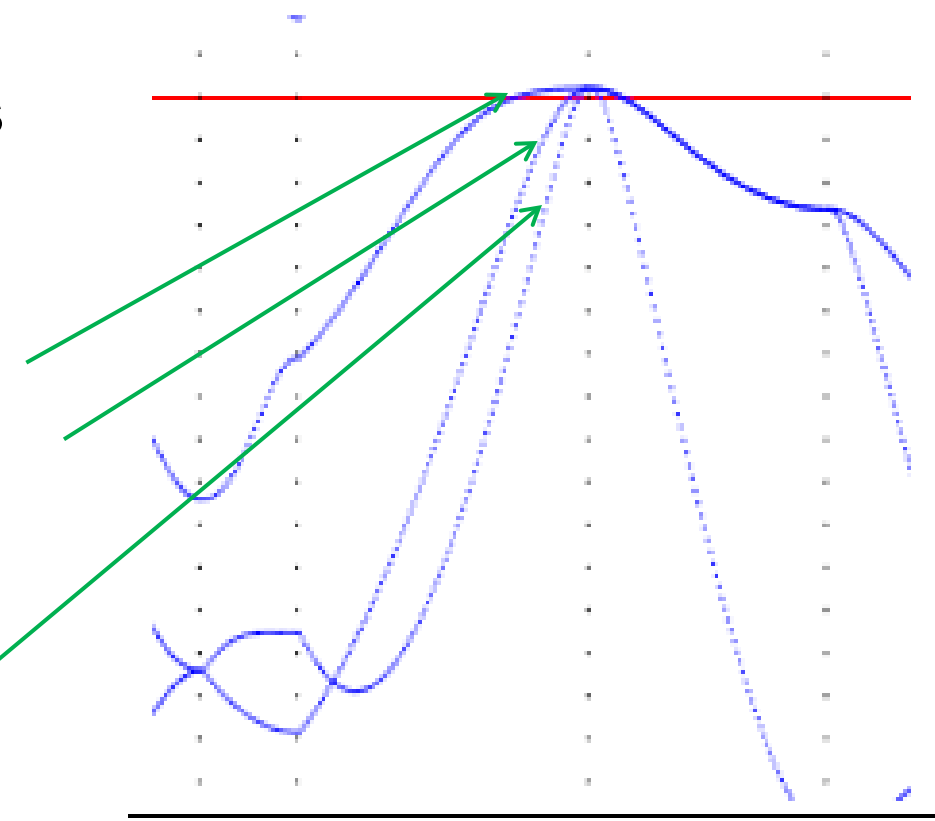
SdH and calculated masses

Γ -K direction - three bands crossing the Fermi level,

0.9-1.2 for external band,

0.11-0.15 for intermediate one

0.03-0.05 for the internal band



W K Γ L

1.2.2 Nanostructuring $Mg_2(Si, Sn)$

Same technique: liquid encapsulation

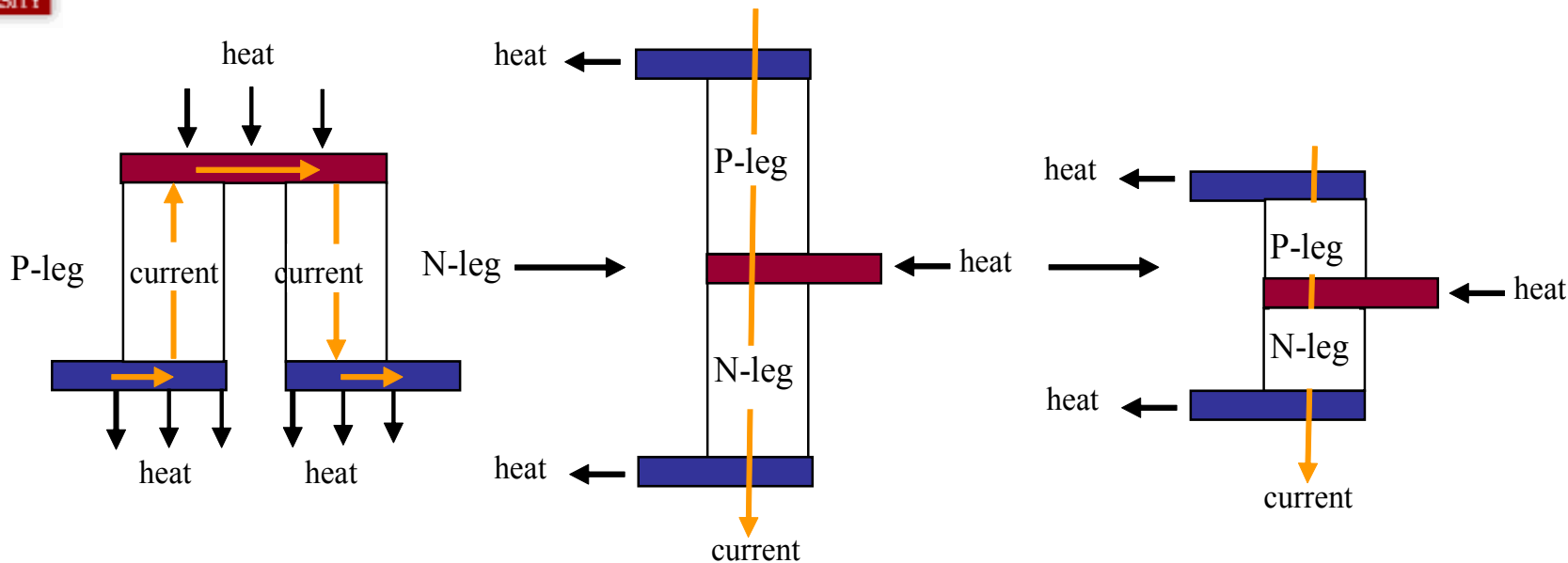
$Mg_2 Si_{1-x}Sn_x/Y$, $Mg_2Si_{1-x}Pb_x/Y$ and $Mg_2Sn_{1-x}Pb_x/Y$ systems

Y as element

Y as compound that do not form compounds with Mg_2X :

- binary silicides
- Binary stannides

2. Thermal Management: new BSST designs



Heat / electrical current in cross-flow geometry

(1) reduced number of interfaces and components

=>reduced parasitic losses

(2)high power density materials => much smaller sizes

(3)segmentation across the specified temperature differential to maximize efficiency

Will be adapted to high-ZT materials & reduced thickness

BSST

3. *Interfaces*

3.1 TE material metallization

3.1.1 Co-pressing of metallized layers and powders during process of Spark Plasma Sintering (SPS)

3.1.2 Post processing of annealed samples and deposition of metals using Physical Vapor Deposition (PVD) methods.

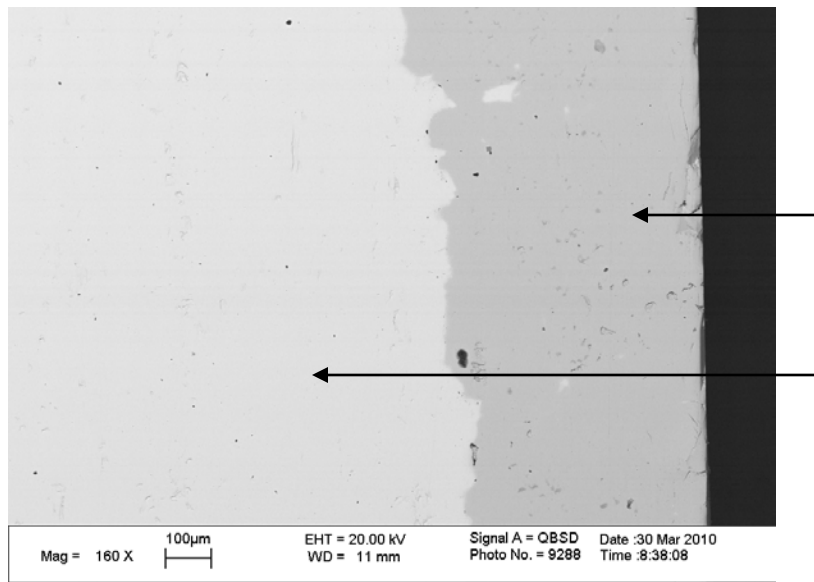
3.2 New compliant device interconnects

3.2.1 Nanosilver

3.2.2 New systems

3.1 TE material metallization

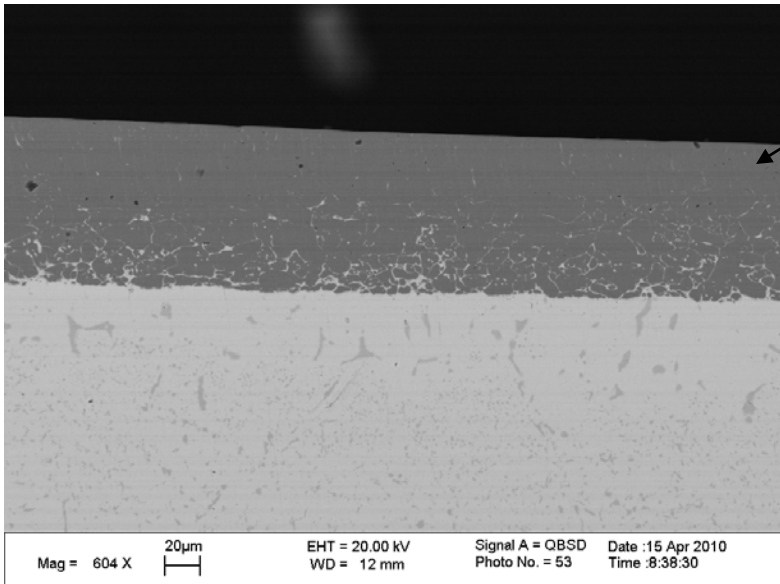
Direct co-sintering during material consolidation (SPS)



400 μm layer of SnTe

p-type PbTe

from powders during Spark Plasma Sintering.



Fe foil co-sintered with p-type PbTe

interdiffusion and likely a eutectic structure

Issues: interdiffusion, diffusion barriers

3.2 Nanosilver interconnect packaging material

Pb-free, high-T die-attach solution:

Binder Surfactant
 Thinner

Surfactant + Organic thinner + Ag nano-powder

- Joint formed below 280°C;
- Melting at 960°C;
- Thermal conduct > 150 W/m-K.



Silver Paste
nanoTach®

Applications:



Uniform
Dispersion



Substrate

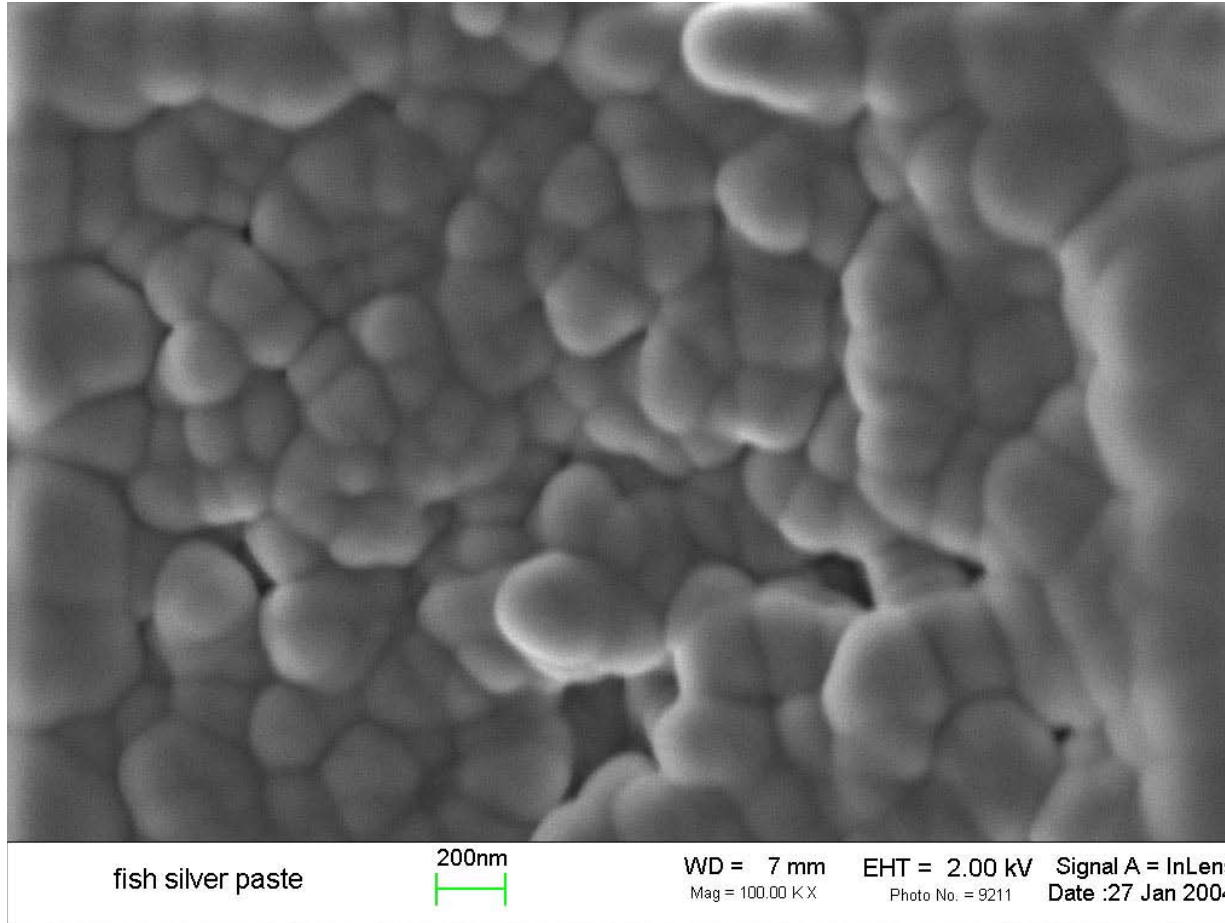
Sintered
joint

Heat up

Cool down

Densification
by diffusion

in situ nanosilver sintering in a scanning electron microscope



30 nm Ag Powder

Properties of nanosilver sintered die-attach compared with the others

	Processing temperature	Max. use temperature	Electrical conductivity $10^5 (\Omega\text{-cm})^{-1}$	Thermal conductivity (W/K·cm)	Die-shear Strength (MPa)
Lead-tin solder	217°C	< 183°C	0.69	0.51	35
Lead-free solder	260°C	< 225°C	0.75	0.70	35
Gold-tin solder	310°C	< 280°C	0.625	0.58	30 - 60
Silver epoxy	100 – 200°C	< 200°C	0.1	0.1	10 – 40
High-Pb solder	340°C	< 280°C	0.45	0.23	15
Hysol® QMI 3555 R	300 – 450°C	<250°C 	6.7×10^{-7}	0.80 	20
		<280°C		<0.8	
Nano-Ag	< 275°C	< 961°C*	3.8	2.4	20 – 40

Nanosilver: developments needed

1. Adapt to thermoelectric materials

Difficulties: Ionic conductivity of silver
especially in chalcogenides

2. Less expensive alternatives

4. Metrology

4.1 TE material characterization exists
OSU, NU, ZTPlus, BSST

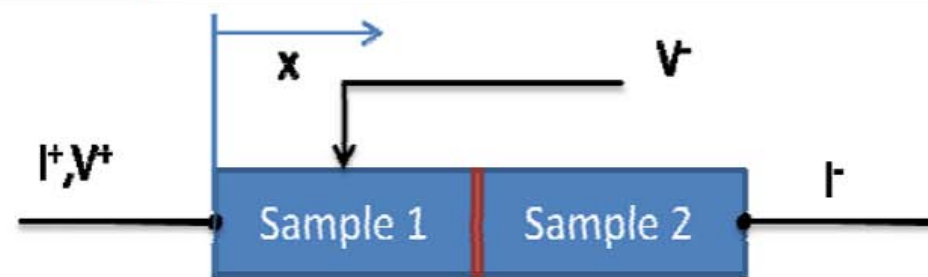
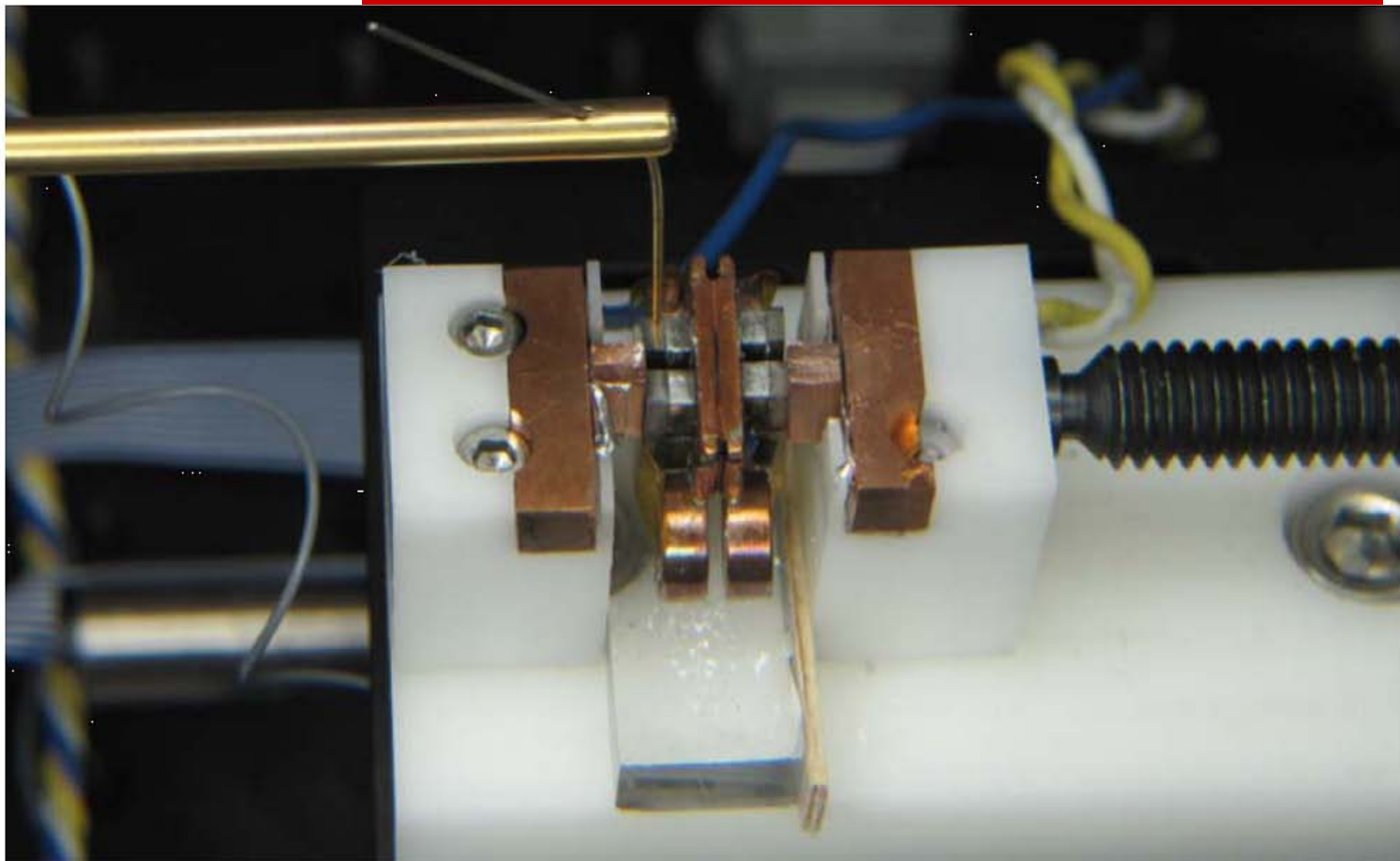
4.2 Electrical contact resistances
ZTPlus

4.3 Thermal contact resistances (new technique)
Virginia Tech

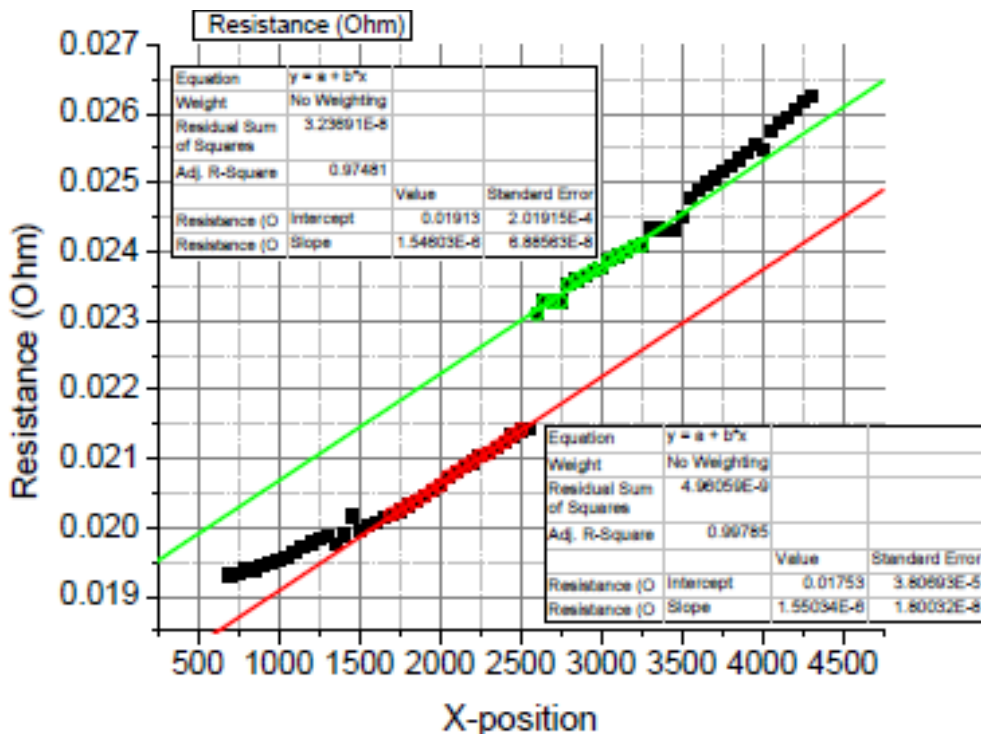
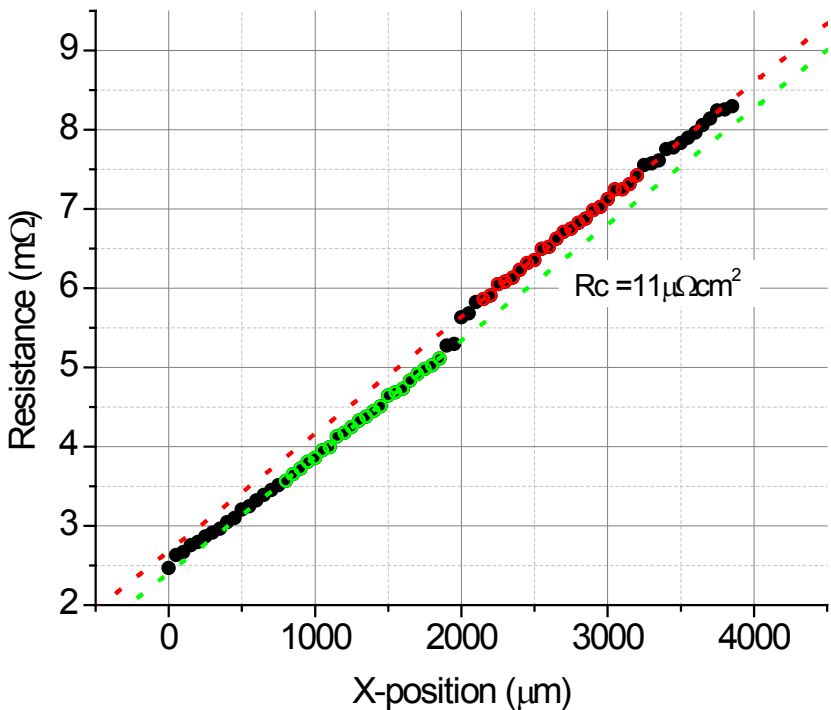
4.4 Device performance
BSST

**4.5 Circular cross-check is now possible
=> determination of the error bars**

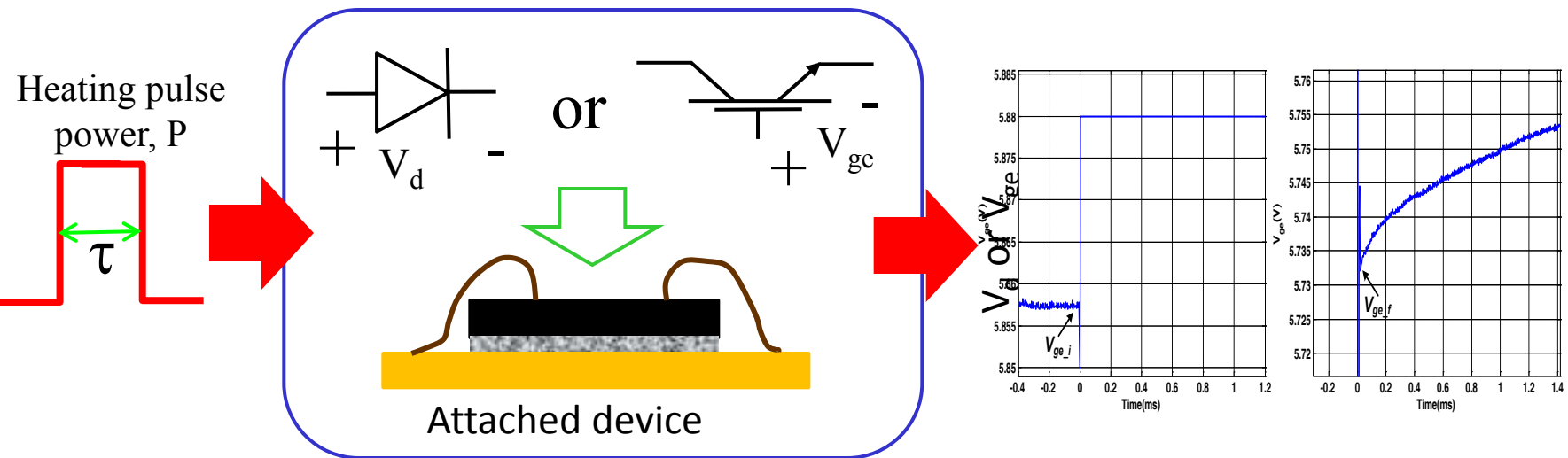
4.1 Electrical contact resistances



4.1 Electrical contact resistances



Thermal impedance characterization of the sintered joints



$$\text{Thermal impedance: } Z_{th} = \frac{\Delta V}{P_H} = \frac{\Delta T}{I_H V_H (1-\varphi)} = \frac{V_{Fi} - V_{Ff}}{I_H V_H (1-\varphi) K}$$

V_{Fi} : The initial VF value before application of heating power;

V_{Ff} : The final VF value after application of heating power;

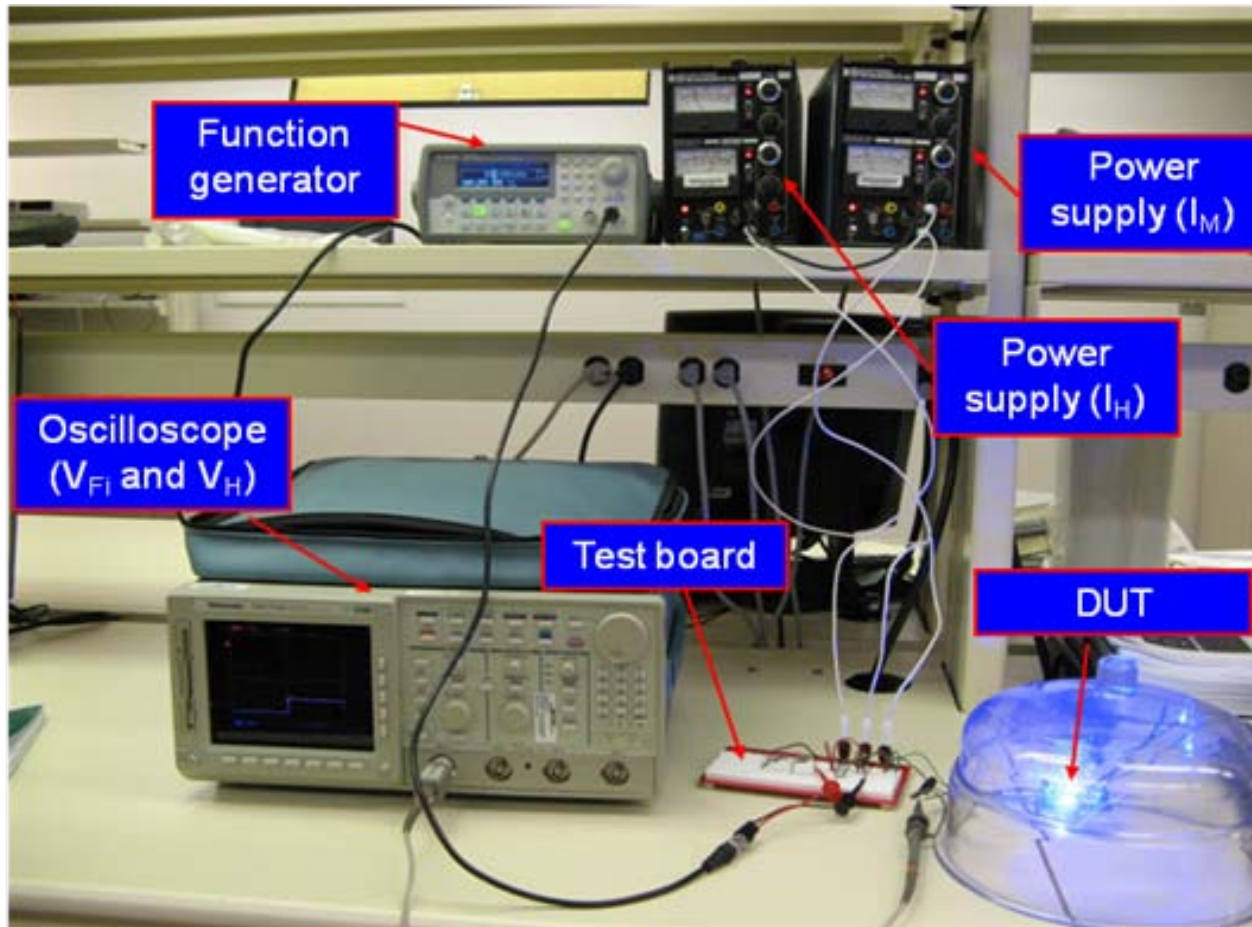
I_H : The current applied to the DUT during the heating time in order to cause power dissipation;

V_H : The heating voltage resulting from the application of I_H to the DUT;

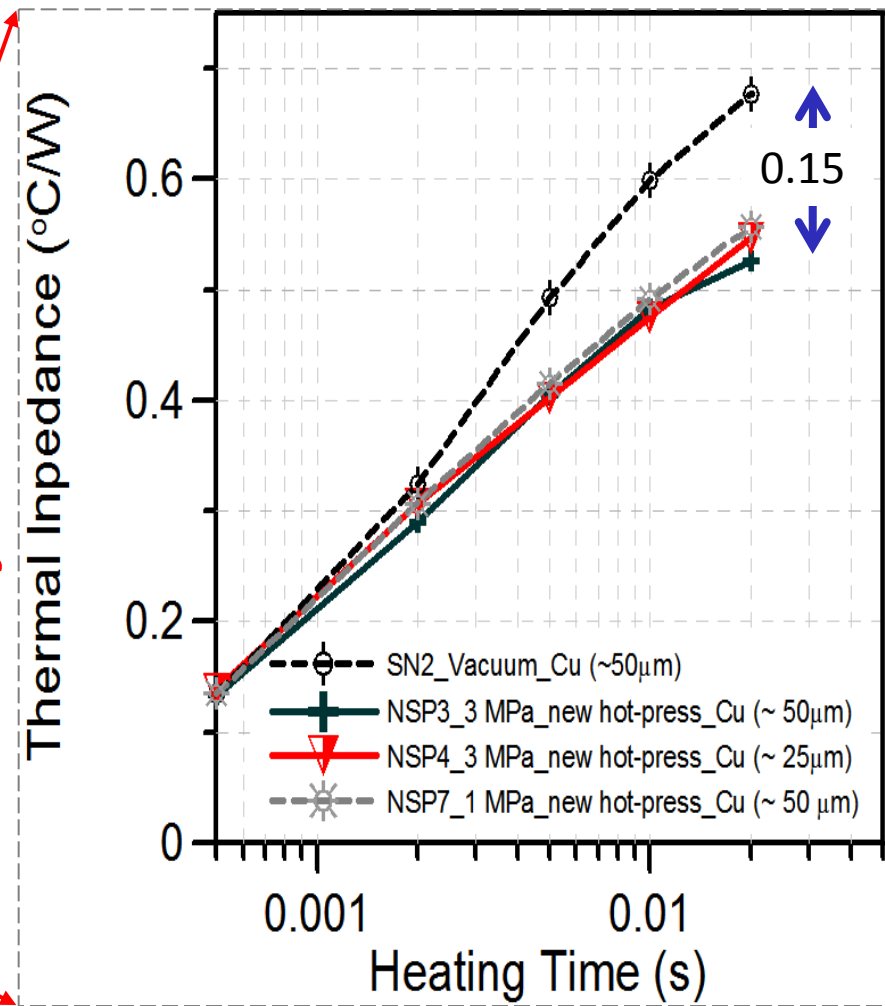
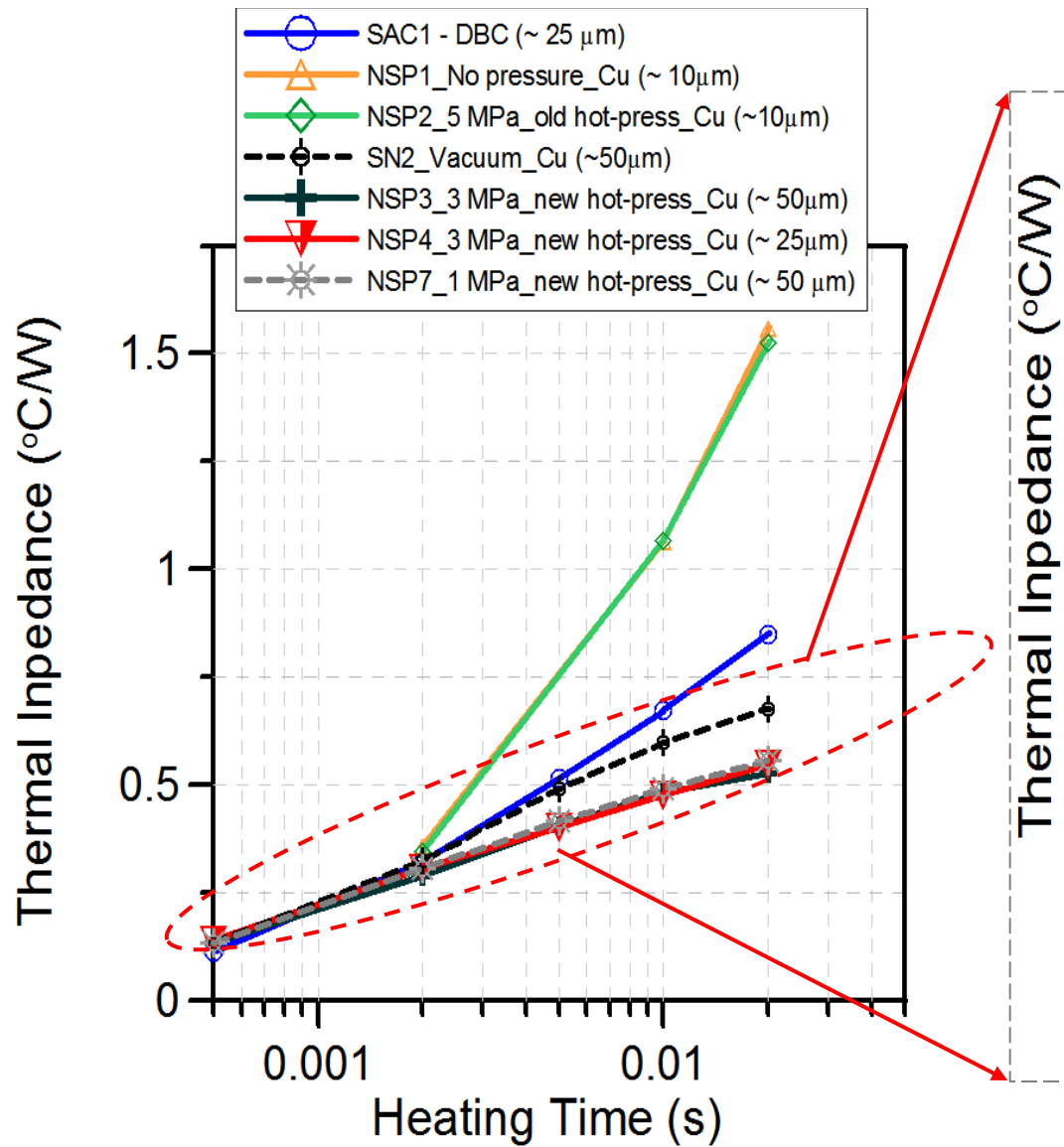
P_H : The heating power pulse magnitude; product of V_H and I_H ;

K : Thermal calibration factor, in mV/ $^{\circ}\text{C}$;

Setup for measuring thermal impedance, Z_{th}



Z_{th} results of a $\sim 20\text{-mm}^2$ IGBT attached by solder and nanosilver



5. Durability

1. Durability is built into every step of the design
2. Extensive durability testing at BSST and ZTPlus

BSST and ZTPlus, have state-of-the-art durability testing facilities used in the development of automotive products.

Ensure that this project incorporates automotive durability standards.

SUMMARY: FIVE THRUSTS

1. New Materials
 1. Two systems: PbSe and Mg₂(Si, Sn)
 2. Two techniques: nanostructuring by liquid encapsulation, resonant levels
2. New thermal design: cross-flow heat and current
3. New Interface technologies
 1. Compliant highly conductive contacts, Ag nanopaste
 2. In-situ metallization during pellet consolidation
 3. Deposition techniques
4. Metrology
 1. New thermal contact resistance measurement technique
 2. Self-consistency check: materials/interfaces/devices
5. Reliability
 1. Design-inherent
 2. Automotive-level durability testing